Dalton Transactions

ROYAL SOCIETY OF CHEMISTRY

PAPER

View Article Online
View Journal | View Issue

Cite this: *Dalton Trans.*, 2025, **54**, 10022

Hierarchical lanthanide-based self-assembly complexes that undergo reversible luminescent response to both temperature changes and chemical reactions within competitive media†

Tumpa Gorai, *‡[a] June I. Lovitt,[a,b] Brendan Twamley,[a] Ena T. Luis [a] and Thorfinnur Gunnlaugsson *[a,c]

Here, we report hierarchical self-assembly formation of a luminescent **Eu^{3+}-1-DPA** complex in mixed aqueous–organic (THF or ethanol) solutions. Its reversible responsive behaviour to temperature change and *in situ* chemical reactions were investigated. The ligands **1-DPA** and **1-DPA-acetate** as well as the Eu(III) complex of **1-DPA**, **Eu^{3+}-1-DPA** were synthesised, and their X-ray crystal structures were determined. The photophysical and material (morphological) properties of the ligands and Eu(III) complexes formed *in situ* of both **1-DPA** and **1-DPA-acetate** were probed in mixed aqueous–organic (THF or ethanol) solutions. The ligands as well as the complexes were shown to aggregate into hierarchical and homogenously formed microspheres and microrods, as demonstrated by carrying out SEM of the drop-cast solutions of these complexes in ethanol–water mixtures. The **Eu^{3+}-1-DPA** complex gave rise to Eu(III)-centred emission [due to deactivation of the $^5D_0 \rightarrow {}^7F_J$ (J = 1–4)]. It showed reversible, thermo-responsive lanthanide-centred emission, while *in situ* esterification using acidic anhydride (forming **Eu^{3+}-1-DPA-acetate**, which was not emissive), and the subsequent NaOH-mediated hydrolysis of the **Eu^{3+}-1-DPA-acetate** assembly induced both Eu(III)-emission and morphological changes, as demonstrated using both spectroscopic and SEM studies.

Received 7th April 2025,
Accepted 22nd May 2025

DOI: 10.1039/d5dt00831j

rsc.li/dalton

Introduction

Developing self-assembly structures from synthetic organic building blocks with the view of generating higher order, or hierarchical self-assemblies, has become an active area of research within supramolecular chemistry.[1] Such an approach can both mimic and help in understanding the properties and the function of naturally occurring hierarchical structures and materials. Non-covalent interactions such as hydrogen bonding,[2] host–guest interactions,[3] donor–acceptor interactions,[4] and metal coordination,[5] have been used (individually or in combination) in the development of a range of functional self-assembly materials.[6] [Ln(III)] is an attractive means to generate such materials, not only because of its unique coordination requirements but also because of its physical properties, such as luminescence and magnetism, which can be transferred to the resulting bulk material. Hence, ions such as Eu(III), Tb(III), and Sm(III) that emit at long wavelengths with line-like emission bands and long excited state lifetimes have been used in the preparation of optoelectronic devices, in up-conversion emission, in chemo- and bio-sensing, probing of chemical processes, in counterfeiting, and in the generation of bio-inspired materials.[7] We reported their use in the development of tuneable luminescent sensors, probes and supramolecular and polymeric gels,[7b,8] as well as in the formation of nanomaterials,[9] and MOFs,[10a] to name just a few. We recently started investigating the use of such ions more generally in the formation of hierarchical assemblies[8,10] that included the use of triple-stranded di-metallic lanthanide helicates. Here, we show that the 3 : 1 (ligand : metal ion) complex **Eu^{3+}-1-DPA** can be employed in the formation of such structures and functional materials. We show that **Eu^{3+}-1-DPA**,[12] in a reversible manner, can respond to both changes in temperature and chemical composition, or a chemical reaction, where **Eu^{3+}-1-DPA** is converted to the corresponding **Eu^{3+}-1-DPA-acetate**, (Scheme 1) upon reacting it with acetic anhydride under mild

[a]*School of Chemistry and Trinity Biomedical Sciences Institute (TBSI), Trinity College Dublin, The University of Dublin, Dublin 2, Ireland. E-mail: gunnlaut@tcd.ie, tumpagorai@gmail.com*
[b]*Advanced Materials and BioEngineering Research (AMBER) Centre, Trinity College Dublin, The University of Dublin, Dublin 2, Ireland*
[c]*Synthesis and Solid State Pharmaceutical Centre (SSPC), Ireland*

†Electronic supplementary information (ESI) available: Experimental details, supporting figures, and crystallography data. CCDC 2427466–2427468. For ESI and crystallographic data in CIF or other electronic format see DOI: https://doi.org/10.1039/d5dt00831j

‡Present address: Department of Polymers and Functional Materials, CSIR-Indian Institute of Chemical Technology, Hyderabad 500007, India.

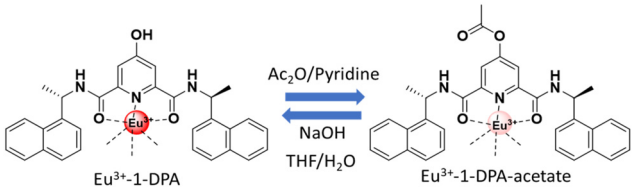

Scheme 1 Reversible conversion of **Eu^{3+}-1-DPA** and **Eu^{3+}-1-DPA-acetate** by *in situ* esterification and hydrolysis reaction.

catalytic conditions, with the reaction being monitored in real time by probing delayed Eu(III) emission. Hence, this work establishes the use of such lanthanide-based hierarchical self-assembly systems as a responsive material in solution.

Results and discussion

Synthesis and characterisation

The **Eu^{3+}-1-DPA** complex was synthesised from the ligand 4-hydroxy-N^2,N^6-bis((*S*)-1-(naphthalen-1-yl)ethyl)pyridine-2,6-dicarboxamide (**1-DPA**), as previously reported by us; in this work, we used **1-DPA** as a starting point for the preparation of several functional lanthanide complexes through functionalisation at the hydroxy position,[12] (see Experimental section and ESI Fig. S1–S3†), and the characterization matched the reported data.[11,12] The **1-DPA-acetate** ligand was also derived from **1-DPA**, by reacting it with acetic anhydride in the presence of pyridine in CH_3CN solution at room temperature for 2 h. The resulting product was fully characterised (ESI Fig. S4–S6†). The ^{1}H NMR (ESI Fig. S4†) showed the characteristic splitting corresponding to the stereogenic centre.

X-ray diffraction analysis was performed for both **1-DPA** and **1-DPA-acetate** ligand crystals (see ESI Fig. S7 and S8,† respectively). The crystal of **1-DPA** was grown from a 1 : 1 DMSO–water solution and was solved in the space group $P2_12_12_1$. The asymmetric unit contained two ligands and two DMSO molecules, with π–π stacking interactions between the pyridine unit and naphthalene unit of two ligands, as well as intramolecular hydrogen bonding between amine N–H and C=O of the amide group of ligands. Each DMSO was H-bonded to the 4-hydroxyl group of **1-DPA**. The crystal structure of **1-DPA-acetate** ligand was obtained from a crystal grown by slow evaporation of a CH_2Cl_2 solution and was solved in the space group $P2_12_12_1$. The asymmetric unit contained two ligands and a disordered solvent: a CH_2Cl_2 molecule at 0.7 occupancy, and a CH_3CN molecule at 0.3 occupancy. There were similar π–π stacking and hydrogen bonding interactions compared with the **1-DPA** ligand.

The corresponding Eu^{3+} complex of **1-DPA**, **Eu^{3+}-1-DPA** was formed by microwave reaction of the ligand in the presence of Eu(III) perchlorate salt in methanol. The crystals were grown by slow diffusion of diethyl ether into a saturated methanol solution of **Eu(1-DPA)$_3$(ClO$_4$)$_3$** complex. The solid-state X-ray crystal structure of **Eu^{3+}-1-DPA** was resolved and demonstrated that the complex was formed in 3 : 1 stoichiometry (Fig. 1). The structure showed each pyridine moiety sandwiched between two naphthalene units, one from each of the other two ligands, resulting in 'forced' π–π stacking, which was absent in the ligand structure and could only be 'forced' upon Eu(III) coordination (see Fig. S9, ESI† for the space filling showing the complete 'engulfing' of the Eu(III) ion by the three ligands). The extended packing is also shown in Fig. 1c, demonstrating highly ordered packing, which was helical in nature. Recently, we showed that such helicity is directly related to the stereochemistry of the ligand, which is transferred to the overall extended structures.[12b] In the case of **Eu^{3+}-1-DPA**, the (*S*,*S*) ligand stereochemistry resulted in a Δ stereochemistry around the Eu(III) ion.

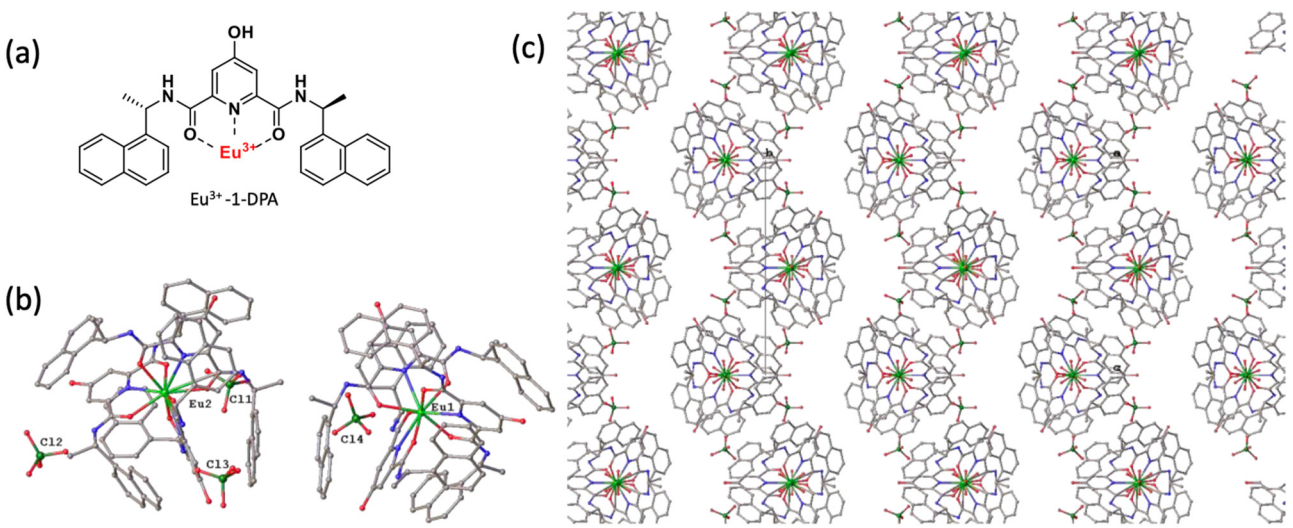

Fig. 1 (a) **Eu^{3+}-1-DPA** complex. (b) Symmetry-generated unit cell, showing one disordered conformation of **1-DPA**'s and ClO_4^- anions. Four unique ClO_4^- sites shown with Cl1 and Cl4 half-occupied. (c) Extended structure and X-ray packing of the **Eu^{3+}-1-DPA** complex showed a wavy layer-like arrangement (see also ESI Fig. S9†).

Photophysical and morphological studies of free ligand 1-DPA and in the presence of Eu(III)

Having synthesised the Eu complex, we next investigated the luminescent and morphological properties of **1-DPA** in the absence and presence of Eu(III).[12] The absorption, fluorescence and excitation spectra of **1-DPA** were recorded in a 50% ethanol/water mixture at room temperature. The ground state displayed a typical absorption band seen for such **DPA**-based systems with two main bands at 220 nm, 280 nm and a hump at ~320 nm (see ESI Fig. S10† for details). Excitation into 280 nm and 320 nm bands resulted in fluorescence emission centred at *ca.* 395 nm (see also ESI Fig. S11†).

The potential aggregation of this ligand was also investigated by carrying out dilution studies, observing both the changes in the absorption and fluorescence emission spectra. In contrast to what was seen in absorption spectra where, with increasing concentration two bands at 280 nm and 320 nm obeyed the Beer–Lambert Law, the emission intensity at 395 nm increased then decreased for λ_{ex} = 280 nm, while the emission intensity at the same wavelength (395 nm) steadily increased for λ_{ex} = 320 nm (see ESI Fig. S11a–d†) with increasing concentration. The fluorescence excitation also reflected a significant change as a function of ligand concentration. Such a redshift in the excitation band is typically caused by aggregation (see ESI Fig. S11e†). We have previously seen such a phenomenon for the formation of microspheres that are formed in mixed aqueous–organic solutions.[1a,b] Hence, we also carried out an investigation into the material properties of this ligand.

The microscopic self-assembly property of **1-DPA** was first investigated in two solvent compositions: water/ethanol (EtOH) and water/tetrahydrofuran (THF) mixtures. The **1-DPA** ligand (1 mM) formed a clear solution in up to 50% water in EtOH and up to 60% water in THF. Scanning electron microscopy (SEM) of the drop-cast and dried samples from these solutions showed the formation of microspheres with average diameters of 0.63 nm and 0.75 nm, respectively, as shown in Fig. 2a (see also ESI: Fig. S12 and S13†), demonstrating their highly uniform morphology.

Next, the assembly was repeated in the presence of 0.1 equivalent of Eu(III) (as $Eu(OAc)_3$) with respect to **1-DPA** which, with the SEM image obtained of the drop-casted solution shown in Fig. 2b, also gave rise to microsphere morphology (see also ESI Fig. S14†). Upon increasing the Eu(III) concentration to 0.2 equivalent, the microspheres underwent association and form a 2D layer-like morphology (Fig. 2c and ESI Fig. S15†). On further increasing Eu(III) to 0.3 equivalent, the spheres gave rise to a close-packing and homogenous morphology (Fig. 2d and see also ESI Fig. S16†). Given that the **DPA** ligand motif forms 1 : 3 complexes with Eu(III), this suggests that the presence of Eu(III) with **1-DPA** gave rise to the formation of uniformly formed self-assembled microspheres that are highly ordered and homogenous in their hierarchical structures.

Next, we investigated the photophysical properties of the **Eu^{3+}-1-DPA** complex and self-assembly material similar to that described above. In EtOH solution, the UV–Vis absorption spectrum gave rise to bands arising from both pyridine as well as naphthalene units (ESI Fig. S17†). Upon excitation into these bands, the Eu(III)-centred emission was apparent due to deactivation of the Eu(III) excited state; $^5D_0 \rightarrow {}^7F_J$ [J = (0) 1–4], demonstrating the sensitisation of the Eu(III) excited state by a ligand (recorded in the phosphorescence mode, *cf.* Fig. 3a). Eu(III) emission could also be observed in the (total) fluorescence emission spectra, as shown in Fig. S23a and S27a.† The Eu(III) electronic-dipole J = 0 transition was also observed (though low in intensity, *cf.* Fig. 3a), signifying that in this complex, the Laporte selection rules were relaxed.[7a,8d]

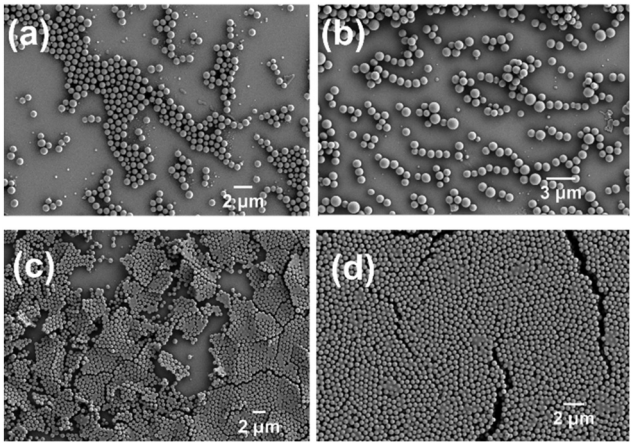

Fig. 2 SEM images of drop-casted and dried (a) **1-DPA**, (b) **1-DPA** with $Eu(OAc)_3$ (0.1 eq.), (c) **1-DPA** with $Eu(OAc)_3$ (0.2 eq.) and (d) **1-DPA** with $Eu(OAc)_3$ (0.3 eq.) solution in 50% H_2O/EtOH.

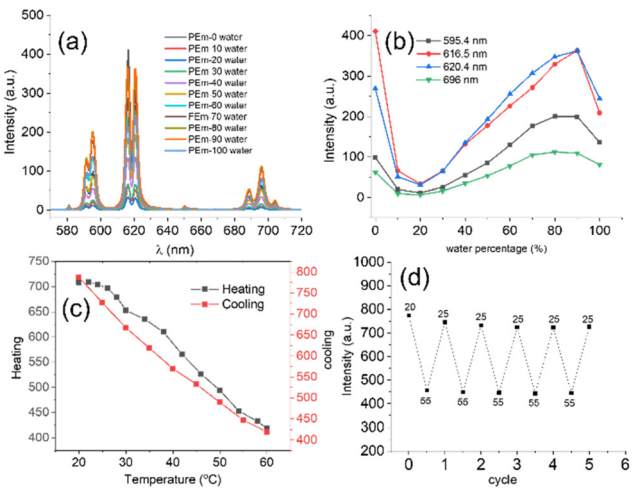

Fig. 3 (a) Variation of emission spectra of the **Eu^{3+}-1-DPA** complex (3.3 μM) for λ_{ex} 281 nm with an increase in water percentage in H_2O/EtOH mixture. (b) Emission change of the **Eu^{3+}-1-DPA** complex (3.3 μM) at 595 nm, 616 nm, 620 nm, and 696 nm with variation in water percentage. (c) Emission change of **Eu^{3+}-1-DPA** (0.33 mM) with heating and cooling, and (d) repeatability of the heating–cooling cycle.

Upon addition of water, a decrease in the absorption centred at 223 nm and 281 nm, respectively, was observed (Fig. S17, ESI†). Concomitantly, Eu(III) emission was also affected, showing a sharp drop upon increasing the percentage of water from 0.45% to 10%, thereafter it showed a gradual increase with increasing water percentage (Fig. 3a and b).

This quenching we assigned to non-radiative deactivation *via* vibrational coupling with water (which is commonly seen for Eu-complexes) as well as a possible contribution from hydrogen bonding involving the three hydroxy moieties in **Eu^{3+}-1-DPA**. Afterwards, emission intensity increased, likely due to increased aggregation of the **Eu^{3+}-1-DPA** complexes and possible removal of water from the aggregated spheres.

Above 90% water, however, a reduction in the emission intensity was again observed. This was most likely due to the formation of larger higher-order aggregates of **Eu^{3+}-1-DPA** in solution, though we cannot say so for certain, because the inner-filter effect can also have a role at such higher concentrations of aggregates. Therefore, from the water percentage-dependent study, we confirmed that 50–60% water/ethanol solvent composition was optimum for a self-assembly study of the **Eu-1-DPA** complex. In this solvent composition range, Eu (III) emission intensity showed a good rise, and the formation of larger aggregates could be omitted. However, prior to that, the changes in Eu(III)-centred emission was also investigated as a function of temperature.

Probing the thermometric luminescence of Eu^{3+}-1-DPA

Many examples of luminescent Eu(III) complexes and polymers have been reported for their thermometric luminescence property.[13] Therefore, having formed the above higher-order systems, we were interested in investigating if indeed **Eu^{3+}-1-DPA** would give rise to such thermo-responsive changes using a 50% H_2O/EtOH solution. Gratifyingly, Eu(III) emission was found to be highly dependent upon temperature, being quenched as a function of gradual heating from 20° C up to 60° C. Moreover, the emission properties were fully reversible, being restored upon cooling back to 20° C (Fig. 3c, see also Fig. S18 ESI†). Furthermore, this 'on–off' emission 'switching' or 'heating–cooling cycle' was repeated five times, as demonstrated in Fig. 3d, with good emission recovery, signifying high stability. This, combined with the changes discussed above in range of aqueous–organic solvent combinations, demonstrate that the complex was stable under these competitive conditions.

Esterification on Eu^{3+}-1-DPA and the concomitant effect on Eu (III) luminescent and morphological properties

Having demonstrated the thermo-responsive emission changes for **Eu^{3+}-1-DPA**, we then investigated if **Eu^{3+}-1-DPA** emission properties could be monitored to observe chemical modification at the 4-hydroxy moiety in **Eu^{3+}-1-DPA.** To demonstrate this, we chose to employ simple esterification and de-esterification reactions, but such reactions have very crucial roles in many (specific and non-specific) biological processes.[14] Moreover, *in situ* esterification and hydrolysis reactions are employed for developing non-equilibrium supramolecular hydrogel formation and self-assembly, which lanthanide ions can also have a major role in.[15] The *in situ* esterification responsive behaviour has, to the best of our knowledge, not been shown for such lanthanide hierarchical self-assemblies before.

For this study, the Eu(III) complex of **1-DPA** and **1-DPA-acetate** were prepared *in situ* in a mixture of 60% H_2O : THF (THF was used to ensure solubility during the acylation reaction) by the addition of aq. $Eu(OAc)_3$ solution, and the Eu(III) emission properties were monitored. The absorption and (total) fluorescence emission spectra (encompassing both **1-DPA** ligand emission and Eu(III) centred emission) of **Eu^{3+}-1-DPA** in this solvent system are shown in Fig. 4a and b, being similar to that observed above.

Therefore, in the case of the **Eu^{3+}-1-DPA** complex formation, the emerging characteristic Eu(III) emission was monitored at 595 nm, 616 nm, and 695 nm in 60% H_2O/THF solution along with the emission band for **1-DPA** ligand at 390 nm (Fig. 4b). However, in the case of the **Eu^{3+}-1-DPA-acetate**, the acetate ligand was found not to sensitize the Eu(III) excited state, and

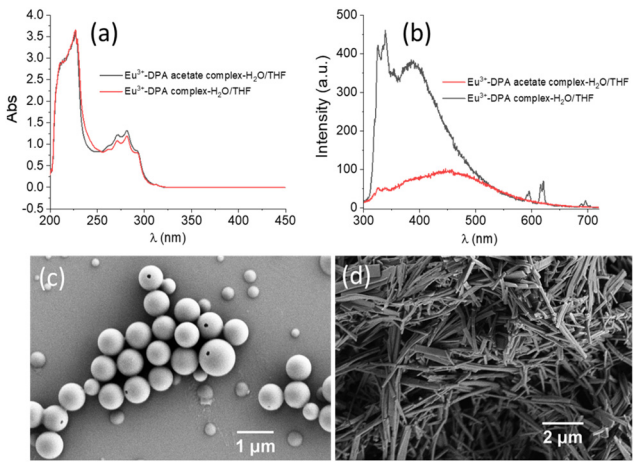

Fig. 4 (a) Absorption and (b) (total) fluorescence emission spectra of the **Eu^{3+}-1-DPA** (33.3 μM) complex and **Eu^{3+}-1-DPA-acetate** (33.3 μM) complex in 60% H_2O/THF for λ_{ex} 281 nm. SEM image of the **Eu^{3+}-1-DPA-acetate** (0.33 mM) complex (c) in 60% H_2O/THF and (d) in 40% H_2O/EtOH.

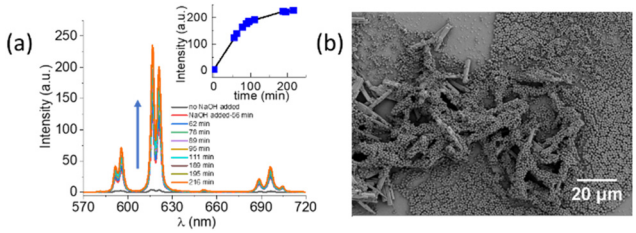

Fig. 5 (a) Increase in the phosphorescence emission of **Eu^{3+}-DPA-acetate** (0.33 mM) complex solution in 50% H_2O/EtOH with time for λ_{ex} 330 nm after addition of NaOH. (b) SEM image of the drop-casted and dried hydrolysis reaction product in 50% H_2O/EtOH.

characteristic peaks for Eu(III) were not observed, Fig. 4b (see also ESI Fig. S19† for phosphorescence spectra). The **Eu^{3+}-1-DPA-acetate** complex (1 mM) was fully soluble in 60% H_2O/THF solution and, upon drop-casting and imaging with SEM, showed a well-defined spherical morphology (*ca.* 0.7 nm) (Fig. 4c) whereas, in 40–50% H_2O/EtOH solution, only a suspension was formed. However, when SEM was done of the drop-casted and dried samples from 50% H_2O/EtOH immediately, and at 30 min, 50 min and 16 h after sample preparation, the **Eu^{3+}-1-DPA-acetate** complex showed a morphological transformation from an entangled particle network to a micro rod-like morphology as the suspension precipitated out of solution (Fig. 4d, see also Fig. S20, ESI†).

Such time-dependent morphological transformations are not commonly reported, but we have recently reported systems based on amino acid-derived BTA ligands,[1a] where such a transformation from particles to fibrous networks was observed with time. These often begin due to formation of thermodynamically driven assembly, though we did not carry out an in-depth investigation into these processes.[16]

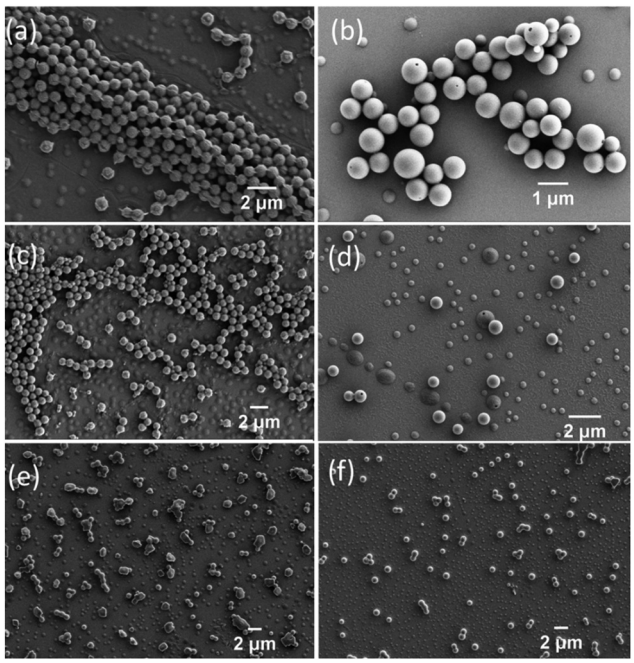

Fig. 6 SEM images of drop-casted and dried samples of (a) the **Eu^{3+}-1-DPA** complex in 60% H_2O/THF, (b) **Eu^{3+}-1-DPA-acetate** complex in 60% H_2O/THF, (c) **Eu^{3+}-1-DPA** complex + pyridine in 60% H_2O/THF and (d–f) **Eu^{3+}-1-DPA** complex + pyridine + acetic anhydride in 60% H_2O/THF solution.

Reversible chemical modification on Eu^{3+}-1-DPA/Eu^{3+}-1-DPA-acetate, and the concomitant effect on Eu(III) luminescent and morphological properties

Having investigated the morphology of **Eu^{3+}-1-DPA-acetate** assembly, we next studied its transformation to **Eu^{3+}-1-DPA**, focusing on base-catalysed ester hydrolysis. As stated above, the **Eu^{3+}-1-DPA acetate** system was non-emissive in 50% H_2O/EtOH solution. However, upon base-catalysed hydrolysis, the Eu(III)-centred emission became apparent over time (upon excitation into the ligand absorption) signifying the formation of the product **Eu^{3+}-1-DPA** (Fig. 5a, see also ESI Fig. S21†). Moreover, morphological investigation of this sample showed the reverse transformation from microrods to aggregated microspheres as the suspension turned into a clear solution (Fig. 5b and Fig. S22, ESI†), further demonstrating the formation of **Eu^{3+}-1-DPA.**

Having achieved the hydrolysis reaction in solution, we next carried out esterification on the luminescent **Eu^{3+}-DPA** complex, in the same manner as described above, using acetic anhydride and pyridine in 50% H_2O : EtOH. However, esterification did not occur, most likely due to the presence of EtOH.

However, when the reaction was performed in 50% H_2O : THF solution, and the changes in the Eu(III) emission were monitored, a sharp quenching was observed within 1 h (Fig. S23, ESI†). Furthermore, slight changes were observed in the UV–Vis absorption spectra as the reaction proceeded,

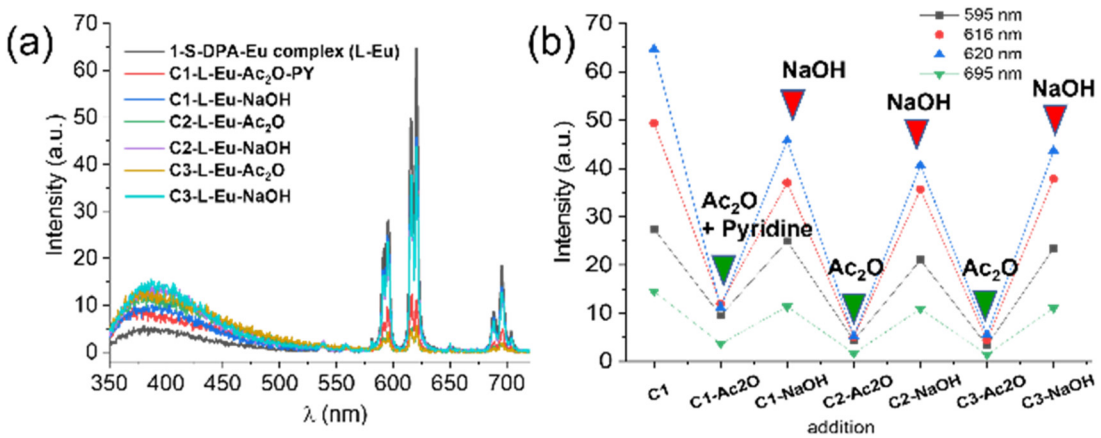

Fig. 7 (a) Emission spectra of the **Eu^{3+}-1-DPA** (0.33 mM) complex upon *in situ* esterification by Ac_2O and pyridine, and hydrolysis by NaOH repeated three times in 60% H_2O/THF. (b) Emission at 595 nm, 616 nm, 620 nm and 695 nm was plotted with each esterification and hydrolysis cycle.

which were consistent with that observed for **Eu^{3+}-DPA-acetate** complex (Fig. S24, ESI†). This indicated that indeed the esterification had been successful.

To further confirm this, the product was isolated, and characterized by ^{1}H NMR spectroscopy (Fig. S25, ESI†) and high-resolution mass spectrometry (HRMS) (Fig. S26, ESI†). Gratifyingly, both techniques confirmed the successful *in situ* formation of the ester. Moreover, carrying out base-catalysed hydrolysis of this product *in situ* resulted in the reformation of **Eu^{3+}-1-DPA** (see Fig. S27, ESI†), with concomitant luminescence enhancements in Eu(III) emission. This was also supported by monitoring the lifetimes of the Eu(III) emission upon these transformations (Fig. S27c and Table S4, ESI†).

As stated above, the products from these reactions were also analysed by SEM (Fig. 6), which showed the expected morphology for both **Eu^{3+}-1-DPA acetate** and **Eu^{3+}-1-DPA** complexes. To study the reversibility of these reactions further, the esterification of **Eu-1-DPA** and concomitant hydrolysis cycles were investigated over three consecutive times in 60% H_2O : THF solutions (Fig. 7). In each case, the addition of pyridine and acetic anhydride to a solution of **Eu^{3+}-1-DPA** resulted in Eu(III) emission quenching (Fig. 7), with the base-catalysed hydrolysis restoring the Eu(III) luminescence. These results further demonstrated the stability of the Eu(III) assembly **Eu^{3+}-1-DPA** in solution, that the *in situ* chemical modification of the system to yield **Eu^{3+}-1-DPA acetate** was possible, and the process was fully reversible over consecutive cycles.

Conclusions

We demonstrated a highly ordered packing arrangement of **Eu-1-DPA** complex crystal, which was reflected in the microscopic dimension as well. Hence, microspheres formed from the self-assembly of the **1-DPA** ligand underwent 2D assembly on Eu(III) complexation with higher uniformity in spheres size. The **Eu^{3+}-1-DPA** complex demonstrated both water-responsive and thermo-responsive emission properties. The *in situ* hydrolysis of **Eu^{3+}-1-DPA acetate** showed morphological transformation from microrods to spheres in EtOH : H_2O solution, which was accommodated with changes in the photophysical properties of these complexes. All these processes were found to be fully reversible. This work is directed towards developing responsive luminescent lanthanide-based hierarchical self-assembled materials for advanced functional investigations.

Experimental

Materials and methods

All solvents and chemicals/reagents were purchased from commercial sources and used without further purification.

Synthesis

4-Hydroxy-N^2,N^6-bis((*S*)-1-(naphthalen-1-yl)ethyl)pyridine-2,6-dicarboxamide (1-DPA). A solution of chelidamic acid monohydrate (1 g, 4.9 mmol) in anhydrous tetrahydrofuran (50 mL) was kept at 0 °C and 1-ethyl-3-(3-dimethylaminopropyl)carbodiimide hydrochloride (EDC·HCl, 2.5 g, 13.0 mmol), 1-hydroxybenzotriazole hydrate (HOBt hydrate, 1.6 g, 11.8 mmol) and *N*,*N*-diisopropylethylamine (DIPEA, 3.8 mL, 21.8 mmol) were added and stirred for 30 min. (*S*)-1-(1-Naphthyl) ethylamine (1.93 mL, 12.0 mmol) was subsequently added and stirred at room temperature for 48 h. THF was removed, and the compound was re-dissolved in dichloromethane (50 mL), washed with 0.1 N HCl (50 mL), aqueous saturated sodium bicarbonate (30 mL) and brine (30 mL). The organic layer was dried over Na_2SO_4, and after removing the solvent under vacuum, the crude product was purified by a flash silica column (24 g, 0–5% MeOH in DCM) to afford **1-DPA** as an off-white solid (1.9 g, 79% yield). ^{1}H NMR (600 MHz, DMSO-D_6) δ ppm: ^{1}H NMR (600 MHz, DMSO) δ 11.41 (s, 1H), 9.39 (d, J = 8.3 Hz, 2H), 8.23 (d, J = 8.4 Hz, 2H), 7.96 (d, J = 8.0 Hz, 2H), 7.86 (d, J = 8.1 Hz, 2H), 7.69 (d, J = 7.1 Hz, 2H), 7.62–7.46 (m, 8H), 5.99 (p, J = 7.1 Hz, 2H), 1.70 (d, J = 7.0 Hz, 6H); ^{13}C NMR(150 MHz, DMSO-D_6) δ ppm: 166.40, 162.77, 151.13, 139.63, 133.46, 130.40, 128.75, 127.52, 126.31, 125.66, 125.44, 123.88, 122.85, 111.95, 44.97, 21.50; HRMS (*m*/*z*) calculated for $C_{31}H_{28}N_3O_3$ [M + H] 490.2131, observed for $C_{31}H_{28}N_3O_3$ [M + H] 490.2129; elemental analysis calculated for $C_{31}H_{27}N_3O_3$. 0.5H_2O, C 74.68, H 5.66, N 8.43, observed C 74.38, H 5.45, O 8.40.

2,6-Bis(((*S*)-1-(naphthalen-1-yl)ethyl)carbamoyl)pyridin-4-yl acetate (1-DPA-acetate). Acetic anhydride (344 μL, 3.67 mmol) and pyridine (295 μL, 3.67 mmol) were added to an acetonitrile solution (3 mL) of **1-DPA** (180 mg, 0.367 mmol) and stirred for 2 h at room temperature. Acetonitrile was removed by evaporation. The reaction mixture was diluted with DCM (30 mL) and washed with water (2 × 30 mL). Dichloromethane was evaporated by rotary evaporation, and the compound was recrystallized from dichloromethane to obtain **1-DPA-acetate** as a crystalline white solid (113 mg, 58% yield). ^{1}H NMR (600 MHz, DMSO) δ ppm: 9.49 (d, J = 8.3 Hz, 1H), 8.23 (d, J = 8.3 Hz, 1H), 8.03–7.99 (m, 1H), 7.97 (d, J = 7.8 Hz, 1H), 7.87 (d, J = 8.2 Hz, 1H), 7.70 (d, J = 7.2 Hz, 1H), 7.62–7.49 (m, 3H), 6.01 (p, J = 7.0 Hz, 1H), 2.33 (s, 1H), 1.73 (d, J = 6.9 Hz, 3H). ^{13}C NMR (150 MHz, DMSO-D_6) δ ppm: 168.17, 162.00, 159.75, 151.46, 139.30, 133.44, 130.38, 128.74, 127.59, 126.32, 125.66, 125.40, 123.13, 122.82, 118.21, 54.84 (CH_2Cl_2), 45.15, 21.38, 20.95; IR ν_{max}(cm^{-1}): 3287.64, 3048.34, 2978.82, 2932.63, 2874.21, 1777.13, 1656.28, 1596.82, 1509.28, 1448.17, 1366.96, 1175.65, 1120.66, 1017.40, 1000.32, 975.98, 907.68, 871.92, 800.44, 774.64, 729.23; HRMS (*m*/*z*) calculated for $C_{33}H_{30}N_3O_4$ [M + H] 532.2231, observed for $C_{33}H_{30}N_3O_4$ [M + H] 532.2239; elemental analysis calculated for $C_{33}H_{29}N_3O_4$. 0.45CH_2Cl_2, C 70.51, H 5.29, N 7.37, observed C 70.48, H 5.25, O 7.35.

Data availability

All data are available upon reasonable request. ESI† is also included with this submission.

Conflicts of interest

There are no conflicts to declare.

Acknowledgements

We thank Science Foundation Ireland (SFI PI Awards 13/IA/1865; SSPC SFI Research Centres Phase 2: 12/RC/2275_P2 to TG), the Irish Research Council (IRC GOIPD/2019/400 to TG and IRC GOIPD/2020/585 to ETL) for financial support. We thank Drs Feeney, Hessman, O'Brien and Ruether for their help with the recording of HRMS and NMR samples.

References

1 (*a*) A. J. Savyasachi, O. Kotova, E. T. Luis, A. D. Lynes, S. Mills, S. A. Bright, G. J. McManus, M. E. Möbius, D. C. Williams, R. Pal, J. J. Boland and T. Gunnlaugsson, *Chem*, 2025, **11**, 102321; (*b*) T. Gorai, J. I. Lovitt, D. I. Umadevi, G. McManus and T. Gunnlaugsson, *Chem. Sci.*, 2022, **13**, 7805–7813; (*c*) A. J. Savyasachi, O. Kotova, S. Shanmugaraju, S. J. Bradberry, G. M. Ó. Máille and T. Gunnlaugsson, *Chem*, 2017, **3**, 764–811; (*d*) J. Chen, F. K. C. Leung, M. C. A. Stuart, T. Kajitani, T. Fukushima, E. Van Der Giessen and B. L. Feringa, *Nat. Chem.*, 2018, **10**, 132–138; (*e*) Y. Sang and M. Liu, *Chem. Sci.*, 2022, **13**, 633–656.

2 (*a*) A. B. Aletti, S. Blasco, S. J. Aramballi, P. E. Kruger and T. Gunnlaugsson, *Chem*, 2019, **5**, 2617–2629; (*b*) T. A. Gudmundsson, G. Kuppadakkath, D. Ghosh, M. Ruether, A. Seddon, R. E. Ginesi, J. Doutch, D. J. Adams, T. Gunnlaugsson and K. K. Damodaran, *Nanoscale*, 2024, **16**, 8922–8930; (*c*) P. A. Korevaar, S. J. George, A. J. Markvoort, M. M. J. Smulders, P. A. J. Hilbers, A. P. H. J. Schenning, T. F. A. De Greef and E. W. Meijer, *Nature*, 2012, **481**, 492–496; (*d*) T. A. Gudmundsson, O. Kotova, S. Barwich, M. E. Möbius and T. Gunnlaugsson, *Chem. – Eur. J.*, 2025, **31**, e202403919.

3 (*a*) O. Kotova, C. O'Reilly, S. T. Barwich, L. E. Mackenzie, A. D. Lynes, A. J. Savyasachi, M. Ruether, R. Pal, M. E. Möbius and T. Gunnlaugsson, *Chem*, 2022, **8**, 1395–1414; (*b*) Y. Zheng, Z. Yu, R. M. Parker, Y. Wu, C. Abell and O. A. Scherman, *Nat. Commun.*, 2014, **5**, 5772.

4 (*a*) A. F. Henwood, N. Curtin, S. Estalayo-Adrián, S. J. Aramballi, T. A. Gudmundsson, J. I. Lovitt, L. C. Sigurvinsson, H. L. Dalton, C. S. Hawes, D. Jacquemin, D. F. O'Shea and T. Gunnlaugsson, *Chem*, 2024, **10**, 578–599; (*b*) L. R. Lázaro, L. C. Sigurvinsson, N. Curtin, J. Ho, E. T. Luis, D. A. McAdams, T. A. Gudmundsson, C. S. Hawes, D. Jacquemin, D. F. O'Shea, E. M. Scanlan, T. Gunnlaugsson and Adam F. Henwood, *J. Mater. Chem. B*, 2025, **13**, 929–942; (*c*) M. Kumar, K. Venkata Rao and S. J. George, *Phys. Chem. Chem. Phys.*, 2014, **16**, 1300–1313.

5 (*a*) J. Xu, J. Wang, J. Ye, J. Jiao, Z. Liu, C. Zhao, B. Li and Y. Fu, *Adv. Sci.*, 2021, **8**, 2101101; (*b*) D. E. Barry, O. Kotova, S. R. Donohoe, N. A. O'Shea, A. J. Savyasachi and T. Gunnlaugsson, *Mater. Chem. Front.*, 2025, **9**, 258–270.

6 (*a*) H. Changshui, Y. Li, Y. Song, Y. Li, H. Liu and D. Zhu, *Adv. Mater.*, 2010, **22**, 3532–3536; (*b*) Z. Chen, C. Dai, W. Xiong, Y. Che and C. Zhang, *Commun. Chem.*, 2021, **4**, 1–7.

7 (*a*) D. E. Barry, D. F. Caffrey and T. Gunnlaugsson, *Chem. Soc. Rev.*, 2016, **45**, 3244–3274; (*b*) O. Kotova, S. J. Bradberry, A. J. Savyasachi and T. Gunnlaugsson, *Dalton Trans.*, 2018, **47**, 16377–16387; (*c*) T. Xian, Q. Meng, F. Gao, M. Hu and X. Wang, *Coord. Chem. Rev.*, 2023, **474**, 214866; (*d*) X. Z. Li, C. Bin Tian and Q. F. Sun, *Chem. Rev.*, 2022, **122**, 6374–6458; (*e*) X. Song, S. Li, H. Guo, W. You, X. Shang, R. Li, D. Tu, W. Zheng, Z. Chen, H. Yang and X. Chen, *Angew. Chem., Int. Ed.*, 2019, **58**, 18981–18986; (*f*) X. Yang, X. Lin, Y. Zhao, Y. S. Zhao and D. Yan, *Angew. Chem., Int. Ed.*, 2017, **56**, 7853–7857; (*g*) K. H. Yim, C. T. Yeung, M. R. Probert, W. T. K. Chan, L. E. Mackenzie, R. Pal, W. T. Wong and G. L. Law, *Commun. Chem.*, 2021, **4**, 2–11; (*h*) E. M. Surender, S. J. Bradberry, S. A. Bright, C. P. McCoy, D. C. Williams and T. Gunnlaugsson, *J. Am. Chem. Soc.*, 2017, **139**, 381–388.

8 (*a*) E. M. Surender, S. J. Bradberry, S. A. Bright, C. P. McCoy, D. Clive Williams and T. Gunnlaugsson, *J. Am. Chem. Soc.*, 2017, **139**, 381–388; (*b*) O. Kotova, R. Daly, C. M. G. dos Santos, M. Boese, P. E. Kruger, J. J. Boland and T. Gunnlaugsson, *Angew. Chem.*, 2012, **124**, 7320–7324; (*c*) M. Martínez-Calvo, O. Kotova, M. E. Möbius, A. P. Bell, T. McCabe, J. J. Boland and T. Gunnlaugsson, *J. Am. Chem. Soc.*, 2015, **137**, 1983–1992; (*d*) E. P. McCarney, J. P. Byrne, B. Twamley, M. Martínez-Calvo, G. Ryan, M. E. Möbius and T. Gunnlaugsson, *Chem. Commun.*, 2015, **51**, 14123–14126.

9 (*a*) S. Comby and T. Gunnlaugsson, *ACS Nano*, 2011, **5**, 7184–7197; (*b*) E. M. Surender, S. Comby, B. L. Cavanagh, O. Brennan, T. C. Lee and T. Gunnlaugsson, *Chem*, 2016, **1**, 438–455.

10 (*a*) E. P. McCarney, C. S. Hawes, J. A. Kitchen, K. Byrne, W. Schmitt and T. Gunnlaugsson, *Inorg. Chem.*, 2018, **57**, 3920–3930; (*b*) D. E. Barry, J. A. Kitchen, K. Pandurangan, A. J. Savyasachi, R. D. Peacock and T. Gunnlaugsson, *Inorg. Chem.*, 2020, **59**, 2646–2650.

11 (*a*) J. P. Leonard, P. Jensen, T. McCabe, J. E. O'Brien, R. D. Peacock, P. E. Kruger and T. Gunnlaugsson, *J. Am. Chem. Soc.*, 2007, **129**, 10986–10987; (*b*) O. Kotova, J. A. Kitchen, C. Lincheneau, R. D. Peacock and T. Gunnlaugsson, *Chem. – Eur. J.*, 2013, **19**, 16181–16186.

12 (*a*) S. J. Bradberry, A. J. Savyasachi, R. D. Peacock and T. Gunnlaugsson, *Faraday Discuss.*, 2015, **185**, 413–431; (*b*) D. F. Caffrey, T. Gorai, B. Rawson, M. Martínez-Calvo, J. A. Kitchen, N. S. Murray, O. Kotova, S. Comby, R. D. Peacock, P. Stachelek, R. Pal and T. Gunnlaugsson, *Adv. Sci.*, 2024, **11**, 2307448.

13 (*a*) R. R. Zairov, A. P. Dovzhenko, S. N. Podyachev, S. N. Sudakova, T. A. Kornev, A. E. Shvedova, A. N. Masliy, V. V. Syakaev, I. S. Alekseev, I. M. Vatsouro, G. S. Mambetova, D. V. Lapaev, I. R. Nizameev, F. Enrichi, A. M. Kuznetsov, V. V. Kovalev and A. R. Mustafina, *Colloids Surf., B*, 2022, **217**, 112664; (*b*) R. Li, F. F. Xu, Z. L. Gong and Y. W. Zhong, *Inorg. Chem. Front.*, 2020, **7**, 3258–3281; (*c*) H. Peng, M. I. J. Stich, J. Yu, L. N. Sun, L. H. Fischer and O. S. Wolfbeis, *Adv. Mater.*, 2010, **22**, 716–719; (*d*) M. T. Berry, P. S. May and H. Xu, *J. Phys. Chem.*, 1996, **100**, 9216–9222; (*e*) J. R. Shakirova, N. N. Shevchenko, V. A. Baigildin, P. S. Chelushkin, A. F. Khlebnikov, O. A. Tomashenko, A. I. Solomatina, G. L. Starova and S. P. Tunik, *ACS Appl. Polym. Mater.*, 2020, **2**, 537–547.

14 B. J. Terry and D. L. Purich, *J. Biol. Chem.*, 1980, **255**, 10532–10536.

15 (*a*) M. P. Helm, C. Wang, B. Fan, M. Macchione, E. Mendes and R. Eelkema, *Angew. Chem., Int. Ed.*, 2020, **59**, 20604–20611; (*b*) J. Boekhoven, W. E. Hendriksen, G. J. M. Koper, R. Eelkema and J. H. Van Esch, *Science*, 2015, **349**, 1075–1079; (*c*) I. N. Hegarty, A. F. Henwood, S. J. Bradberry and T. Gunnlaugsson, *Org. Biomol. Chem.*, 2023, **21**, 1549–1557; (*d*) I. N. Hegarty, S. J. Bradberry, J. I. Lovitt, J. M. Delente, N. Fox, R. Daly and T. Gunnlaugsson, *Mater. Chem. Front.*, 2023, **7**, 906–916.

16 (*a*) A. Aliprandi, M. Mauro and L. De Cola, *Nat. Chem.*, 2016, **8**, 10–15; (*b*) L. Zhang, X. Wang, T. Wang and M. Liu, *Small*, 2015, **11**, 1025–1038.